

What Programmable Vector Fields Can (and Cannot) Do: Force Field Algorithms for MEMS and Vibratory Plate Parts Feeders

Karl-Friedrich Böhringer Bruce Randall Donald
Robotics & Vision Laboratory
Department of Computer Science
Cornell University, Ithaca, NY 14853

Noel C. MacDonald
School of Electrical Engineering and
Cornell Nanofabrication Facility
Cornell University, Ithaca, NY 14853

URL <http://www.cs.cornell.edu/home/karl/MicroManipulation>

Abstract

Programmable vector fields can be used to control a variety of flexible planar parts feeders. These devices can exploit exotic actuation technologies such as arrayed, massively-parallel microfabricated motion pixels or transversely vibrating (macroscopic) plates. These new automation designs promise great flexibility, speed, and dexterity—we believe they may be employed to orient, singulate, sort, feed, and assemble parts. However, since they have only recently been invented, programming and controlling them for manipulation tasks is challenging.

When a part is placed on our devices, the programmed vector field induces a force and moment upon it. Over time, the part may come to rest in a dynamic equilibrium state. We demonstrate lower bounds (i.e., impossibility results) on what the devices cannot do, and results on a classification of control strategies yielding design criteria by which well-behaved manipulation strategies may be developed. We suggest sufficient conditions for programmable fields to induce well-behaved equilibria on every part placed on our devices. We define composition operators to build complex strategies from simple ones, and show the resulting fields are also well-behaved. We discuss whether fields outside this class can be useful and free of pathology.

Using these tools, we describe new manipulation algorithms. In particular, we improve existing planning algorithms by a quadratic factor, and the plan-length by a linear factor. Using our new and improved strategies, we show how to simultaneously orient and pose any part, without sensing, from an arbitrary initial configuration. We relax earlier dynamic and mechanical assumptions to obtain more robust and flexible strategies.

Finally, we consider parts feeders that can only implement a very limited “vocabulary” of vector fields. We discuss the tradeoff between mechanical complexity and planning complexity.

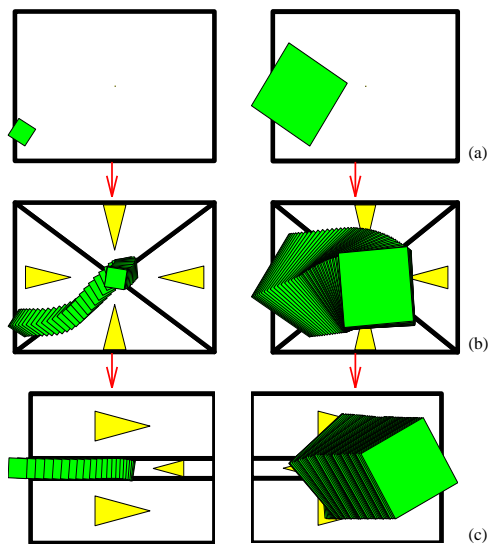


Figure 1: Sensorless sorting using force vector fields: Parts of different sizes are first centered and subsequently separated depending on their size.

1 Introduction

Programmable vector fields can be used to control a variety of flexible planar parts feeders. These devices often exploit exotic actuation technologies such as arrayed, microfabricated motion pixels [5, 4] or transversely vibrating plates [1]. These new automation designs promise great flexibility, speed, and dexterity—we believe they may be employed to orient, singulate, sort, feed, and assemble parts (see for example Figures 1 and 4). However, since they have only recently been invented, programming and controlling them for manipulation tasks is challenging. Our research goal is to develop a science base for manipulation using programmable vector fields.

When a part is placed on our devices, the programmed vector field induces a force and moment upon it. Over time, the part may come to rest in a dy-

dynamic equilibrium state. In principle, we have tremendous flexibility in choosing the vector field, since using modern array technologies, the force field may be programmed pixel-wise. Hence, we have a lot of control over the resulting equilibrium states. By chaining together sequences of vector fields, the equilibria may be cascaded to obtain a desired final state—for example, this state may represent a unique orientation or pose of the part.

We pose the question *Which vector fields are suitable for manipulation strategies?* In particular, we ask whether the fields may be *classified*. That is: can we characterize all those vector fields in which every part has stable equilibria? While this question has been well-studied for a point mass in a field, the issue is more subtle when lifted to a body with finite area, due to the moment covector. To answer, we first demonstrate impossibility results, in the form of “lower bounds:” there exist perfectly plausible fields which induce *no* stable equilibrium in very simple parts.

Fortunately, there is also good news. We suggest conditions for fields to induce well-behaved equilibria when lifted, by exploiting the theory of potential fields. While potential fields have been widely used in robot control [11, 14, 13], micro-actuator arrays present us with the ability to *explicitly* program the applied force *at every point* in a vector field. Whereas previous work has developed control strategies with *artificial* potential fields, our fields are non-artificial (i.e., physical). This alone makes our application of potential field theory unique and novel. Moreover, such fields can be composed using addition, sequential composition, “parallel” composition by superposition of controls, or by a new kind of “morphing” of control signals which we will define.

Finally, the desire to implement complicated fields raises the question of control uncertainty. We close by describing how families of potential functions can be used to represent control uncertainty, and analyzed for their impact on equilibria, and we will give an outlook on still open problems and future work.

2 Experimental Apparatus: Parts Feeders

The most common type of parts feeder is the *vibratory bowl feeder*, where parts in a bowl are vibrated using a rotary motion, so that they climb a helical track. As they climb, a sequence of baffles and cutouts in the track create a mechanical “filter” that causes parts in all but one orientation to fall back into the bowl for another attempt at running the gauntlet [6].

The reason for the success of vibratory bowl feeders and the Sony APOS system [10] is the underlying principle of *sensorless manipulation* [8] that allows parts positioning and orienting without sensor

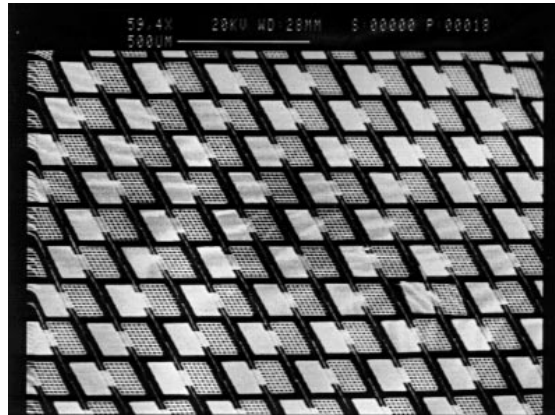


Figure 2: A prototype M-CHIP fabricated in 1995. A large unidirectional actuator array (scanning electron microscopy). Each actuator is $180 \times 240 \mu\text{m}^2$ in size. Detail from a 1 in^2 array with more than 11,000 actuators. For more pictures on device design and fabrication see URL <http://www.cs.cornell.edu/home/karl/MicroActuators>.

feedback. This principle is even more important at small scales, because sensor data will be less accurate and more difficult to obtain. The APOS system or bowl feeders are unlikely to work in the micro domain: instead novel device designs for micro-manipulation tasks are required. The theory of sensorless manipulation is the science base for developing and controlling such devices.

2.1 Microfabricated Actuator Arrays

A wide variety of micromechanical structures (devices with features in the μm range) has been built recently by using processing techniques known from VLSI industry. In our actuator array design, each unit device consists of a rectangular grid etched out of single-crystal silicon suspended by two rods that act as torsional springs (Figure 2). The grid is about $200 \mu\text{m}$ long and extends $120 \mu\text{m}$ on each side of the rod. The rods are $150 \mu\text{m}$ long. The current asymmetric design has $5 \mu\text{m}$ high protruding tips on one side of the grid that make contact with an object lying on top of the actuator. The other side of the actuator consists of a denser grid above an aluminum electrode. If a voltage is applied between silicon substrate and electrode, the dense grid above the electrode is pulled downward by the resulting electrostatic force. Simultaneously the other side of the device (with the tips) is deflected out of the plane by several μm . Hence an object can be lifted and pushed sideways by the actuator.

Because of its low inertia (resonance in the high kHz range) the device can be driven in a wide frequency range from DC to several 100 kHz AC. Our actuators need not be operated at resonance: They can also be

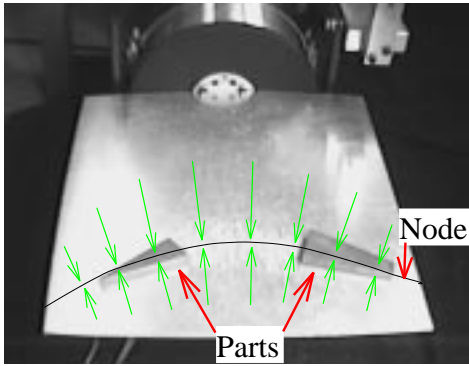


Figure 3: Vibratory parts feeder: an aluminum plate (size $50\text{ cm} \times 40\text{ cm}$) exhibits a vibratory minimum. Parts are attracted to this *nodal line* and reach equilibrium there. See also URL <http://www.cs.cornell.edu/home/karl/VibratoryAlign>. Reproduced with permission from [1].

served to periodically “hit” an object on top, hence applying both lateral and vertical forces. Our calculations and experiments have shown that the force generated with a torsional actuator is approximately $50\text{ }\mu\text{N}$, which corresponds to a force-per-area ratio of $200\text{ }\mu\text{N}/\text{mm}^2$, large enough to levitate e.g. a piece of paper ($1\text{ }\mu\text{N}/\text{mm}^2$) or a silicon wafer ($10\text{ }\mu\text{N}/\text{mm}^2$).

The fabrication process and mechanism analysis are described in more detail in [5, 4].

2.2 Macroscopic Vibratory Parts Feeder

Böhringer et al. [1] have presented a device that uses the force field created by transverse vibrations of a plate to position and align parts. The device consists of an aluminum plate that is attached to a commercially available electrodynamic vibration generator. For low amplitudes and frequencies, the plate moves longitudinally with no perceptible transverse vibrations. However, as the frequency of oscillations is increased, transverse vibrations of the plate become more pronounced. The resulting motion is similar to the forced transverse vibration of a rectangular plate, clamped on one edge and free along the other three sides. This vibratory motion creates a force field in which particles are attracted to locations with minimal vibration, called the *nodal lines*. This field can be programmed by changing the frequency, or by employing clamps as programmable fixtures that create various vibratory nodes.

Figure 3 shows two parts, shaped like a triangle and a trapezoid, after they have reached their stable poses. To better illustrate the orienting effect, the curve showing the nodal line has been drawn by hand. *Nota bene*: This device can only use the finite manipulation grammar described in Section 6.2 since it can only generate a constrained set of vibratory patterns, and cannot implement radial strategies.

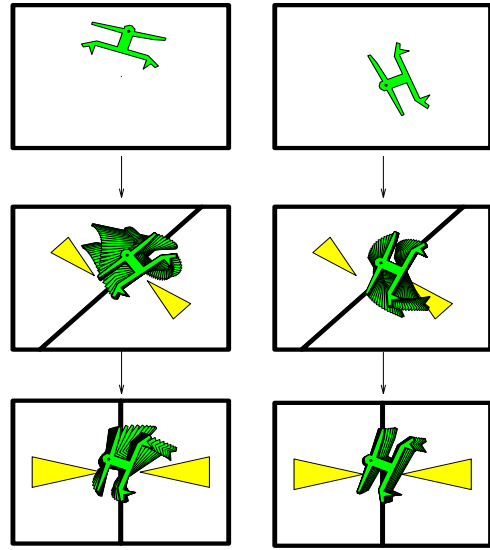


Figure 4: Sensorless parts alignment using force vector fields: The part reaches unique orientation after two subsequent squeezes. There exist such alignment plans for all polygonal parts. See URL <http://www.cs.cornell.edu/home/karl/MicroManipulation> for an animated simulation.

3 Equilibrium Analysis For Programmable Vector Fields

For the generation of manipulation plans with programmable vector fields it is essential to be able to predict the motion of a part in the field. Particularly important is determining the stable equilibrium poses a part can reach in which all forces and moments are balanced. This *equilibrium analysis* was described in our previous paper [5], where we presented a theory of manipulation for programmable vector fields, and an algorithm that generates manipulation plans to orient polygonal parts without sensor feedback using a sequence of *squeeze fields*.

We now briefly review the algorithm in [5], since the tools developed there are essential to understanding our improved results.

3.1 Planning of Manipulation Strategies

In [5] we proposed a family of control strategies called *squeeze fields* and a planning algorithm for parts-orientation.

Definition 1 [5] *Assume l is a straight line through the origin. A squeeze field F is a two-dimensional force field defined as follows: (1) If $z \in \mathbb{R}^2$ lies on l then $F(z) = 0$. (2) If z does not lie on l then $F(z)$ is the unit vector normal to l and pointing towards l .*

We refer to the line l as the *squeeze line*, because l lies in the center of the squeeze field. See Figure 4 for examples of squeeze fields.

Assuming quasi-static motion, a small object will move perpendicularly towards the line l and come to rest there. We are interested in the motion of an arbitrarily shaped (not necessarily small) part P . Let us call P_1, P_2 the regions of P that lie to the left and to the right of l , respectively, and C_1, C_2 their centers of gravity. In a rest position both translational and rotational forces must be in equilibrium. We obtain the following two conditions:

I: The areas P_1 and P_2 must be equal.

II: The vector $C_2 - C_1$ must be normal to l .

P has a motion component normal to l if **I** does not hold. P has a rotational motion component if **II** does not hold.

Definition 2 A part P is in force equilibrium if the forces acting on P are balanced. P is in moment equilibrium if the moments acting on P are balanced. Total equilibrium is simultaneous force and moment equilibrium.

Let (x_0, y_0, θ_0) be an equilibrium pose of P . (x_0, y_0) is the corresponding translation equilibrium, and θ_0 is the corresponding orientation equilibrium.

To model our actuator arrays and vibratory devices, in [5] we made the following assumptions:

DENSITY: The generated forces can be described by a vector field, i.e. the individual microactuators are dense compared to the size of the moving part.

2PHASE: The motion of a part has two phases: (1) Pure translation towards l until the part is in force equilibrium. (2) Motion in force equilibrium until moment equilibrium is reached.

Note that due to the elasticity and oscillation of the actuator surfaces, we can assume continuous area contact, and not just contact in three or a few points. Relaxing assumption 2PHASE is one of the key results of this paper.

The main result of [5] is summarized in the following Theorem (see Figure 4):

Theorem 3 [5] For a connected polygonal part P and an actuator array \mathcal{A} there exists an alignment strategy $\mathcal{S} = (l_1, \dots, l_k)$ that uniquely orients P up to symmetries.

This scheme may be generalized to the case where l is slightly curved, as in the “node” of the vibrating plate in Figure 3. See [1] for details.

The remaining sections of this paper investigates using more exotic fields (not simple squeeze patterns) to (1) relax assumption 2PHASE, (2) reduce the planning complexity, (3) reduce the number of equilibria, (4) reduce the execution complexity (plan length), and (5) determine feasibility results and limitations for manipulation with general force fields.

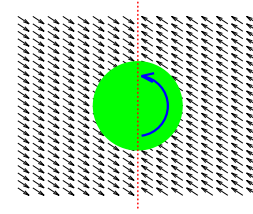


Figure 5: Unstable part in the skewed squeeze field. The disk with center on the squeeze line will keep rotating. Moreover, it has *no* stable equilibrium in this field.

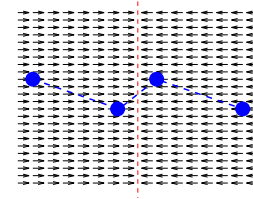


Figure 6: S-shaped part with four rigidly connected point-contact “feet” in unstable total equilibrium (forces and moments balance). There exists *no* stable equilibrium position for this part in a vector field with a simple squeeze pattern.

4 Lower Bounds: What Programmable Vector Fields Cannot Do

We now present “lower bounds” — constituting vector fields and parts with pathological behavior, making them unusable for manipulation. These counterexamples show that we must be careful in choosing programmable vector fields, and that, *a priori*, it is not obvious when a field is well-behaved.

In Section 3 we saw that in a vector field with a simple squeeze pattern (see again Figure 4), polygonal parts reach certain equilibrium poses. This raises the question of a *general classification of all those vector fields in which every part has stable equilibria*. There exist vector fields that do not have this property even though they are very similar to a simple squeeze.

Proposition 4 A skewed vector field induces no stable equilibrium on a disk-shaped part.

Proof: Consider Figure 5: Only when the center of the disk coincides with the center of the squeeze pattern do the translational forces acting on the disk balance. But it will still experience a positive moment that will cause rotation. \square

Similarly we would like to identify the *class of all those parts that always reach stable equilibria* in particular vector fields. From Section 3 we know that connected polygons in simple squeeze fields satisfy this condition. This property relies on finite area contacts:

it does not hold for point contacts. As a counterexample consider the part in Figure 6.

Proposition 5 *There exist parts that do not have stable equilibria in a simple squeeze field.*

Proof: The S-shaped part in Figure 6 has four rigidly connected “feet” with small contact surfaces. As the area of each of these four feet approaches zero, the part has *no* stable equilibrium in a simple squeeze field. There is only one orientation for the part in which both force and moment balances out, and this orientation is unstable. \square

Finally, the *number of stable equilibria* of a given part influences both the planning complexity and the plan length of an alignment strategy. It also affects the resolution of the vector field that is necessary to perform a strategy accurately. Even though practically all parts we have considered exhibit only one or two equilibria, there exist no tight bounds on the maximum number of equilibria.

Proposition 6

- A. *Regular polygons with n vertices have $\Omega(n)$ stable orientation equilibria in a squeeze field.*
- B. *Every connected polygon has $O(n^2)$ stable orientation equilibria in a squeeze field.*

There exist simple polygons with n vertices that can be bisected by a straight line in up to $O(n^2)$ topologically different ways [2]. This suggests that there could be parts that have $\Omega(n^2)$ equilibria in a squeeze field, which would imply alignment plans of length $\Omega(n^2)$ and planning complexity $\Omega(n^4)$.

While the counterexample in Figure 6 may be plausibly avoided by prohibiting parts with “point contacts,” the other examples (Figure 5 and Proposition 6B) are more problematic. In Section 5, we show how to choose programmable vector fields that exclude some of these pathological behaviors, by using the theory of potential fields to describe a class of force vector fields for which *all* polygonal parts have stable equilibria. In Section 6.1, we show how to combine these fields to obtain new fields in which all parts have only $O(n)$ equilibria.

To summarize: We can show that the separating field shown in Figure 1c is not a potential field, and that there exist parts that will spin forever, without equilibrium, in this field (this follows by generalizing the construction in Figure 5). However, for *specific parts*, such as those shown in Figure 1, this field is useful if we can pose the parts appropriately first (e.g., using the potential field shown in Figure 1b).

5 Completeness: Classification Using Potential Fields

In this section we give a family of vector fields that will be useful for manipulation tasks. These fields be-

long to a specific class of vector fields: the class of fields that have a potential.

We are interested in a *general classification of all those vector fields in which every part has stable equilibria*. As motivation, recall that a skewed vector field, even though very similar to a regular squeeze pattern (see again Figure 4), induces *no* stable equilibrium in a disk-shaped part (Figure 5).

Consider the class of vector fields on \mathbb{R}^2 that have a *potential*, i.e. fields F in which the work is independent of the path, or equivalently, the work on any closed path is zero, $\oint F \cdot ds = 0$. In a potential field each point (x, y) is assigned a real value $U(x, y)$ that can be interpreted as its potential energy. When U is smooth, then the vector field F associated with U is the gradient $-\nabla U$. In general, $U(x, y)$ is given, up to an additive constant, by the integral $\int_{\alpha} F \cdot ds$ (when it exists and it is unique), where α is an arbitrary path from a fixed reference point (x_0, y_0) to (x, y) .

An ideal point object is in stable equilibrium iff it is at a local minimum of U .

Definition 7 *For a part P of arbitrary shape we define the lifted potential $U_P : \mathcal{C} \rightarrow \mathbb{R}$, where $\mathcal{C} = \mathbb{R}^2 \times S^1$ is the configuration space of P . U_P is the area integral of the potential U over P in configuration (x, y, θ) .*

Again, $U_P(x, y, \theta)$ can be interpreted as the potential energy of part P in configuration (x, y, θ) .

One can show that the category of potential fields is closed under the operation of lifting. Therefore we obtain a lifted potential field U_P whose local minima are the stable equilibrium configurations in \mathcal{C} for part P . Furthermore, potential fields are closed under addition. We can thus create and analyze more complex fields by looking at their components. In general, the theory of potential fields allows us to classify manipulation strategies with vector fields, offering new insights into equilibrium analysis and providing the means to determine strategies with stable equilibria. For example, it allows us to show that equilibrium in a simple squeeze field is equivalent to the stability of a homogeneous boat floating in water.

Example: Radial fields. A *radial field* is a vector field whose forces are directed towards a specific center point. It can be used to center a part in the plane. The field in Figure 1b can be understood as a radial field with a rather coarse discretization using only four different force directions. Note that this field has a potential.

As a specific example for radial fields, consider the *unit radial field* R which is defined by $R(\underline{x}) = -\underline{x}/\|\underline{x}\|$ for $\underline{x} \neq 0$, and $R(0) = 0$. Note that R has a discontinuity at the origin. A smooth radial field can be defined,

for example, by $R'(\underline{x}) = -\underline{x}$. The corresponding potential fields are $U(\underline{x}) = \|\underline{x}\|$, and $U'(\underline{x}) = \frac{1}{2}\|\underline{x}\|^2$, respectively. Note that U is continuous (but not smooth), while U' is smooth.

Counterexample: Skewed squeeze fields. Consider again the *skewed squeeze field* in Figure 5. This is not a potential field, which explains why the disk-shaped part has no equilibrium: Note that for example the integral on a cyclic path along the boundary of the disk is non-zero.

Example: Morphing and combining vector fields. Our strategies from [5] (see Section 3) have *switch points* in time where the vector field changes discontinuously (Figure 4). This is because we have shown that after one squeeze, for every part, the orientation equilibria form a finite set of possible configurations, but in general there exists no unique equilibrium. Hence subsequent squeezes are needed to disambiguate the part orientation. Therefore these switches are necessary for strategies with squeeze patterns.

One may ask whether, using another class of potential field strategies, *unique* equilibria may be obtained without discrete switching. We believe that *continuously varying* vector fields of the form $(1-t)F + tG$, where $t \in [0, 1]$ represents time, and F and G are squeezes, may lead to vector fields that have this property. Here “+” denotes point-wise addition of vector fields, and we will write “ $F \rightsquigarrow G$ ” for the resulting continuously varying field. By restricting F and G to be fields with potentials U and V , we know that $U + V$ and $(1-t)U + tV$ are potential fields, and hence we can guarantee that $F + G$ and $F \rightsquigarrow G$ are well-behaved strategies. These form the basis of our new algorithms in Section 6.

Complete Potential Fields. So far we have presented specific force fields that do (squeeze and radial fields) or do not (skewed squeeze fields) induce stable equilibria on certain classes of parts. We conclude this section by suggesting a criterion that provides a sufficient condition on force fields such that all parts of a certain size reach a stable equilibrium. Recall that for a region $R \subset \mathbb{R}^2$ with boundary ∂R , the set $\partial R \oplus B_d(0)$ includes all points that are within a distance d from ∂R . The complement of this set is denoted as $CI(B_d(0), R) = R - (\partial R \oplus B_d(0))$.

Definition 8 Consider a force field F with potential U defined on a convex set R . U is d -upward-shaped if the following condition holds: For every point $s \in (\partial R \oplus B_d(0)) \cap R$, there does not exist an $\alpha \in \mathbb{R}^+$ such that $F(s) = \alpha(s' - s)$ for any $s' \in \partial R \cap B_d(s)$.

Hence within the boundary region $\partial R \oplus B_d(0)$ of R , a force field F with upward-shaped potential U does not have any forces that point towards the boundary.

Conjecture 9 Consider a force field F defined on a convex set R , and a connected polygonal part P . Let d be the smallest diameter of a circle that circumscribes P . F induces stable equilibria for the part P if: (1) F has a d -upward-shaped potential U . (2) When P is initially placed into the force field F , its center of mass lies within the region $CI(B_d(0), R)$. (3) The motion of P in F is governed by first-order dynamics.

The use of potential fields will be invaluable for the analysis of effective and efficient manipulation strategies, as discussed in the following section. In particular, it will be useful for proving the completeness of a manipulation planner.

6 New and Improved Manipulation Algorithms

The part alignment strategies in Section 3.1 have *switch points* in time where the vector field changes discontinuously (Figures 1 and 4). We can denote such a *switched strategy* by $F_1 * F_2 * \dots * F_s$, where the F_i are vector fields. In Section 3.1 we recalled that a strategy to align a (non-convex) polygonal part with n vertices may need up to $O(n^2)$ switches, and require $O(n^4)$ time in planning. To improve these bounds, we now consider a broader class of vector fields including simple squeeze patterns, radial, and combined fields as described in Section 5.

In Section 6.1 we show how, by using radial and combined vector fields, we can significantly reduce the complexity of the plans from that of Section 3. In Section 6.2 we describe a general planning algorithm that works with a limited “grammar” of vector fields (and yields, correspondingly, less favorable complexity bounds).

6.1 Radial Strategies

Some force fields exhibit rotational symmetry properties that can be used to generate efficient manipulation strategies:

Property 10 Let P be a connected polygonal part in a force field F . There exists a unique pivot point v such that P is in stable equilibrium iff v coincides with $(0, 0)$.

Now consider the connected polygonal part P in an ideal radial force vector field R as described in Section 5.

Proposition 11 In a unit radial field R , Property 10 holds.

Proof: See our corresponding techreport [3]. \square

Surprisingly, v need not be the center of area of P . For example, consider a large and a small square

connected by a long rod of negligible width. The pivot point of this part will lie inside the larger square. But if the rod is long enough, the center of area will lie outside of the larger square. However, the following corollary holds:

Corollary 12 *For a part P in a continuous radial force field R' given by $R'(\underline{x}) = -\underline{x}$, the pivot point of P coincides with the center of area of P .*

Proof: The force acting on P in R' is given by $F = \int_P -\underline{x} dA$, which is also the formula for the (negated) center of area. \square

Now, suppose that R is combined with a simple squeeze pattern S , which is scaled by a factor $\delta > 0$, resulting in $R + \delta S$. The squeeze component δS of this field will cause the part to align with the squeeze, similarly to the strategies in Section 3.1. But note that the radial component R keeps the part centered in the force field. Hence, by keeping R sufficiently large (δ small), we can assume that the pivot point of P remains within an ϵ -ball of the center of R . This implies that assumption 2PHASE is no longer necessary. Moreover, ϵ can be arbitrarily small by an appropriate choice of δ .

Proposition 13 *For a connected polygon with n vertices there are at most $O(n)$ stable equilibria in a field of the form $R + \delta S$ if δ is sufficiently small and positive.*

Proof: See our corresponding techreport [3]. \square

In analogy to Goldberg's algorithm [9], we obtain plans for unique part alignment (and positioning) of length $O(n)$. They can be computed in time $O(n^2)$. The resulting plan for parts positioning is of the form $(R + \delta S_1) * \dots * (R + \delta S_{O(n)})$. Compared to the old algorithm in Section 3.1 it improves the plan length by a factor of n , and the planning complexity is reduced by a factor of n^2 . The planner is complete: For any polygonal part, there exists a plan of the form $*_i(R + \delta S_i)$. Moreover, the algorithm is guaranteed to find a plan for any input part. By appending a step which is merely the radial field R without a squeeze component, we are guaranteed that the part P will be uniquely posed (v is at the origin) as well as uniquely oriented. We can also show that the continuously varying "morphing" strategy $(R + \delta S_1) \rightsquigarrow \dots \rightsquigarrow (R + \delta S_{O(n)}) \rightsquigarrow R$ works in the same fashion to achieve the same unique equilibrium.

6.2 Manipulation Grammars

The development of devices that generate programmable vector fields is still in its infancy. The existing prototype devices exhibit only a limited range of programmability. For example, the prototype MEMS

arrays described in Section 2.1 [5, 4] currently have actuators in only four different directions, and the actuators are only row-wise controllable. Arrays with individually addressable actuators at various orientations are possible (see [5, 12, 4]) but require significant development effort. There are also limitations on the resolution of the devices given by fabrication constraints. For the vibrating plate device from Section 2.2 the fields are even more constrained by the vibrational modes of the plate.

We are interested in the capabilities of such constrained systems. In this section we give an algorithm that decides whether a part can be uniquely positioned using a given set of vector fields, and it synthesizes an optimal-length plan if one exists. If we think of these vector fields as a vocabulary, we obtain a language of manipulation plans. We are interested in those expressions in the language that correspond to a plan for uniquely posing the part.

The elements of our "manipulation grammar" are (sequences of) vector fields that bring the part into a *finite* set of possible equilibrium positions. From Section 6.1 we know that combined radial-squeeze patterns $R + \delta S$ have this property. However, there are simpler fields that also have this finiteness property, for example two combined non-parallel squeezes $F+G$, or a sequence of two orthogonal squeezes $F * F_{\perp}$. That is: For any polygonal part P , either of these examples is *always* guaranteed to reduce P to a *finite* set of equilibria in its configuration space $C = \mathbb{R}^2 \times S^1$.

Proposition 14 *Consider a polygonal part P , and m force fields $\{F_i\}$, $1 \leq i \leq m$, with at most k distinct equilibria in the configuration space C for P in each field F_i . There is an algorithm that generates an optimal-length plan to uniquely pose P up to symmetries, if such a plan exists. This algorithm runs in $O(m^2 k (s(n) + 2^k))$ time, where $s(n)$ is a function of the complexity of polygon P (with n vertices). If no such plan exists, the algorithm will signal failure.*

Proof: See our corresponding techreport [3]. \square

Hence, as in [8], for any part we can decide whether a part can be uniquely posed using the field vocabulary $\{F_i\}$ but (a) the planning time is exponential and (b) we do not know how to characterize the class of parts that can be oriented by $\{F_i\}$. However, the resulting plans are optimal in size.

This result illustrates a tradeoff between mechanical complexity (the dexterity and controllability of field elements) and planning complexity (the computational difficulty of synthesizing a strategy). If one is willing to build a device capable of radial fields, then one reaps great benefits in planning and execution speed. On the other hand, we can still plan for simpler devices (see Figure 3), but the plan synthesis is more expensive, and we lose some completeness properties.

7 Conclusions and Open Problems

Geometric Filters. This paper focuses mainly on sensorless manipulation strategies for *unique positioning* of parts. Another important application of programmable vector fields are *geometric filters*. Figure 1 shows a simple filter that separates smaller and larger parts. We are interested in the question *Given n parts, does there exist a vector field that will separate them into specific equivalence classes?* For example, does there exist a field that moves small and large rectangles to the left, and triangles to the right? In particular, it would be interesting to know whether for any two different parts there exists a sequence of force fields that will separate them.

Uncertainty. In practice, neither the force vector field nor the part geometry will be exact, and both can only be characterized up to tolerances [7]. This is particularly important at micro scale. Within the framework of potential fields, we can express this uncertainty by considering not one single potential function U_P , but rather *families of potentials* that correspond to different values within the uncertainty range. Bounds on part and force tolerances will correspond to limits on the variation within these function families. An investigation of these limits will allow us to obtain upper error bounds for manipulation tasks under which a specific strategy will still achieve its goal.

Discrete Force Fields. For the manipulation strategies described in this paper we assume that the force fields are continuous, i.e. that the generated forces are dense compared to the moving part (assumption DENSITY in Section 3.1). When manipulating very small parts on microactuator arrays, this condition may be only approximately satisfied. We are interested in the limitations of the continuous model, and we would like to know the conditions under which it is necessary to employ a different, discrete model of the array that takes into account individual actuators, as well as the gaps between actuators.

Acknowledgments

We thank Danny Halperin and Lydia Kavradi for useful discussions and valuable comments, and Jean-Claude Latombe for his hospitality during our stay at the Stanford Robotics Laboratory.

Support is provided in part by the NSF under grants No. IRI-8802390, IRI-9000532, IRI-9201699, and by a Presidential Young Investigator award to Bruce Donald, in part by NSF/ARPA Special Grant for Experimental Research No. IRI-9403903, and in part by the AFOSR, the Mathematical Sciences Institute, Intel Corporation, and AT&T Bell laboratories. This work was supported by ARPA under contract DABT 63-69-C-0019. The device fabrication was performed at the Cornell Nanofabrication

Facility (CNF), which is supported by the NSF grant ECS-8619049, Cornell University, and Industrial Affiliates.

References

- [1] K.-F. Böhringer, V. Bhatt, and K. Y. Goldberg. Sensorless manipulation using transverse vibrations of a plate. In *Proc. IEEE Int. Conf. on Robotics and Automation (ICRA)*, pages 1989 – 1996, Nagoya, Japan, May 1995. .
- [2] K.-F. Böhringer, B. R. Donald, and D. Halperin. The area bisectors of a polygon and force equilibria in programmable vector fields, 1996. In preparation.
- [3] K.-F. Böhringer, B. R. Donald, and N. C. MacDonald. New and improved manipulation algorithms for MEMS arrays and vibratory parts feeders: What programmable vector fields can (and cannot) do — Part II. Technical report, Cornell University, Robotics and Vision Laboratory, Ithaca, NY, Oct. 1995. .
- [4] K.-F. Böhringer, B. R. Donald, and N. C. MacDonald. Single-crystal silicon actuator arrays for micro manipulation tasks. In *Proc. IEEE Workshop on Micro Electro Mechanical Systems (MEMS)*, San Diego, CA, Feb. 1996. .
- [5] K.-F. Böhringer, B. R. Donald, R. Mihailovich, and N. C. MacDonald. Sensorless manipulation using massively parallel microfabricated actuator arrays. In *Proc. IEEE Int. Conf. on Robotics and Automation (ICRA)*, pages 826–833, San Diego, CA, May 1994. .
- [6] G. Boothroyd, C. Poli, and L. E. Murch. *Automatic Assembly*. Marcel Dekker, Inc., 1982.
- [7] B. R. Donald. *Error Detection and Recovery in Robotics*, volume 336 of *Lecture Notes in Computer Science*. Springer Verlag, Berlin, 1989.
- [8] M. A. Erdmann and M. T. Mason. An exploration of sensorless manipulation. *IEEE Journal of Robotics and Automation*, 4(4), Aug. 1988.
- [9] K. Y. Goldberg. Orienting polygonal parts without sensing. *Algorithmica*, 10(2/3/4):201–225, August/September/October 1993.
- [10] H. Hitakawa. Advanced parts orientation system has wide application. *Assembly Automation*, 8(3), 1988.
- [11] O. Khatib. Real time obstacle avoidance for manipulators and mobile robots. *Int. Journal of Robotics Research*, 5(1):90–99, Spring 1986.
- [12] W. Liu and P. Will. Parts manipulation on an intelligent motion surface. In *IROS*, Pittsburgh, PA, 1995.
- [13] J. Reif and H. Wang. Social potential fields: A distributed behavioral control for autonomous robots. In K. Goldberg, D. Halperin, J.-C. Latombe, and R. Wilson, editors, *Algorithmic Foundations of Robotics*, pages 431–459. K. Peters, Wellesley, MA, 1995.
- [14] E. Rimon and D. Koditschek. Exact robot navigation using artificial potential functions. *IEEE Transactions on Robotics and Automation*, 8(5), October 1992.